J. Fluid Mech. (1986), *vol.* 172, *pp.* 513–529
Printed in Great Britain

Weakly nonlinear Kelvin–Helmholtz waves

By JOHN W. MILES

Institute of Geophysics and Planetary Physics, University of California, San Diego, La Jolla, CA 92093, USA

(Received 31 January 1986)

The Lagrangian L for gravity waves of finite amplitude in an N-layer, stratified shear flow is constructed as a functional of the generalized coordinates $\boldsymbol{q}_\nu(t) \equiv \{q_n^\nu(t)\}$ of the $N+1$ interfaces, where the q_n^ν are the Fourier coefficients in the expansion of the interfacial displacement $\eta_\nu(\boldsymbol{x}, t)$ in a complete, orthogonal set $\{\psi_n(\boldsymbol{x})\}$. The explicit expansion of L is constructed through fourth-order in the q_n^ν and $\dot{q}_n^\nu$. Progressive interfacial waves and Kelvin–Helmholtz instability in a two-layer fluid are examined, and the earlier results of Drazin (1970), Nayfeh & Saric (1972) and Weissman (1979) are extended to finite depth. It is found that the pitchfork bifurcation associated with the critical point for Kelvin–Helmholtz instability, which is supercritical for infinitely deep layers, may be subcritical (inverted) for finite depths. The evolution equations that govern Kelvin–Helmholtz waves in the parametric neighbourhood of this critical point are shown to be equivalent to those for a particle in a two-parameter, central force field. The effect of surface tension is examined in an Appendix. Finally, the wave motion forced by flow over a sinusoidal bottom (as in Thorpe's tilting tank) is examined and the corresponding resonance curves and Hopf bifurcations determined. Numerical integrations reveal that stable limit cycles exist in some parametric neighbourhoods of these bifurcations. Period doubling was observed but did not lead to chaotic motion.

1. Introduction

I consider here a Lagrangian formulation for weakly nonlinear gravity waves in an N-layer, stratified, inviscid, incompressible shear flow with special reference to the Kelvin–Helmholtz problem for a two-layer fluid of finite depth. The formulation follows that for internal waves in a stratified fluid (Miles 1986); in particular, a velocity potential exists for each layer by virtue of the uniformity of both density and velocity therein. Surface tension, which is omitted in the body of the text, is incorporated in Appendix A.

Weakly nonlinear Kelvin–Helmholtz (K–H) waves in an unbounded fluid have been considered previously by Drazin (1970), Maslowe & Kelly (1970), Nayfeh & Saric (1972), Weissman (1979) and Saffman & Yuen (1982). Full nonlinearity has been examined by Saffman & Yuen (1982) and Yuen (1984), using numerical methods. The present work is closely related to that of Drazin, Nayfeh & Saric and Weissman.

Drazin (1970) focuses on the transition to K–H instability and imposes the Boussinesq approximation. He includes surface tension, but the Boussinesq approximation suppresses the effects of a possible resonance between a gravity-capillary wave and its second harmonic. He deduces from Squire's theorem that waves moving

in the direction of the basic flow are more unstable than oblique waves and therefore dominate the transitional régime [but this does not hold for strong nonlinearity (Yuen 1984)]. He examines the possible limit cycles in the transitional régime on the hypotheses of slowly varying amplitude and constant phase and concludes that they are stable.

Nayfeh & Saric (1972) extend Drazin's (1970) work by eschewing the Boussinesq approximation and allowing for spatial, as well as temporal, modulation. They first consider stable progressive wave, extending the results of Maslowe & Kelly (1970) by obtaining the second-order modification of the wave speed. They then consider the K–H stability problem for wavenumbers close to that of the minimum wave speed (for which gravity and capillarity are equally important). They examine two classes of limit cycles in the transitional régime on the hypotheses of slowly varying amplitude and constant phase and find that capillarity may render one of these classes unstable.

Weissman (1979), like Nayfeh & Saric, allows for both spatial and temporal modulation and focuses on the neighbourhood of K–H instability. He gives extensive results for wave packets, including, for example, solitary waves. Proceeding from the same hypotheses as those of Nayfeh & Saric, he finds four (in contrast to one/two for Drazin/Nayfeh & Saric) classes of limit cycles.

I begin the present development, in §2, by extending my earlier calculation of the Lagrangian for a laterally unbounded, N-layer fluid to incorporate uniform flows in the individual layers, which are characterized by their depths, densities and velocities, d_ν, ρ_ν and U_ν, $\nu = 1, 2, \ldots, N$. I expand the displacement of the νth interface and the velocity potential in the νth layer in the complete set of normal modes $\exp(i\boldsymbol{k}_n \cdot \boldsymbol{x})$, determine the coefficients in the expansion of the velocity potential, ϕ_ν, in terms of the modal amplitudes of its bounding interfaces through the variational requirement $\delta\mathscr{L}/\delta\phi_\nu \equiv 0$, and neglect terms of fifth and higher order in the modal amplitudes in the Lagrangian (in keeping with the hypothesis of weak nonlinearity). In §3, I apply the general formulation to two-dimensional progressive waves at the interface of a two-layer fluid with rigid upper and lower boundaries, for which the first approximation has the form $\eta = A\cos k(x-ct)$, where $c = c(k)$ is determined by the usual K–H dispersion relation. Weak nonlinearity generates a second harmonic of the form $kA^2\cos 2k(x-ct)$ and augments the wave speed by a term proportional to Ck^2A^2, where the dimensionless parameter C may be either positive or negative. The present results extend those of Nayfeh & Saric (1972) by providing the dependence of C on the layer depths; in particular, they reveal that C, which is positive-definite for gravity waves on an interface between layers of depth much larger than the wavelength, may be negative for sufficiently shallow layers. (As Nayfeh & Saric were the first to point out, it also may be negative for capillary-gravity waves on an interface between infinitely deep layers.) This result, which is not unexpected, corresponds to that of Keulegan & Carpenter (1961) for internal waves.

In §4, I examine the parametric neighbourhood of K–H instability for an arbitrarily prescribed wavenumber (in contrast to the formulations of Nayfeh & Saric and Weissman, wherein the wavenumber is assumed to approximate that of the minimum wave speed for a capillary-gravity interfacial wave). The end result is a pair of second-order differential equations for the slowly varying amplitude and phase of the marginally stable (or unstable) interfacial wave. These normalized equations contain two parameters: β, which is a measure of proximity to the neutral curve *in* the parameter space, and γ, which is the sign of the aforementioned parameter C at the proximate point on the neutral curve. They are analogous to the

equations governing the motion of a particle in a central force field that is described by β and γ. They are integrable in terms of elliptic functions, but the stable motions are only quasi-periodic (the periods of the amplitude and phase are unequal), in consequence of which the phase-space trajectories are not closed. These results generalize those of Drazin (1970), Nayfeh & Saric (1972) and Weissman (1979), all of whom obtain integrals only for the special case of constant phase, for which the motion is simply periodic.

The progressive wave of §3 is a fixed point of the differential equations of §4 in a three-dimensional phase space (the phase angle in the four-dimensional phase space being ignorable). It is stable for all amplitudes (subject to $kA \ll 1$) if $C > 0$, but only for a limited range of amplitudes if $C < 0$.

These last conclusions remain valid in the presence of weak (linear) damping, which I introduce in §4. However, damping renders the evolution equations non-integrable.

In §5, I consider the stationary wave forced by flow of a two-layer fluid over a sinusoidal bottom, as in the experiments of Thorpe (1968) and Altman (1985).† There then is a third parameter, α, which measures an appropriately defined mean value of U (which is eliminated in §4 through transformation to a reference frame moving with that mean velocity). I also include damping, which introduces a fourth parameter, δ. The resonance curve of amplitude versus β is triple-valued in some range of β if $|\alpha|\delta$ is sufficiently small and comprises both stable and unstable fixed points of the corresponding evolution equations. The intermediate branch, which lies between the turning points of the triple-valued curve, is unstable, just as in the case of a linearly damped Duffing oscillator (Stoker 1950, pp. 90–96). The upper/lower branch is stable for $\gamma = \pm 1$, but, in contrast to the Duffing analogue, the lower/upper branch may comprise both stable and unstable fixed points. The division between stable and unstable fixed points *on* these branches are Hopf bifurcations, of which there may be 0, 1, 2 or 3. Numerical integration of the evolution equations for the slowly varying amplitude and phase reveal that limit cycles may emerge from these Hopf bifurcations. The numerical integrations also revealed period doubling and quadrupling in the parametric evolution of the limit cycles for $\gamma = +1$ (although not for $\gamma = -1$), but neither period-doubling cascades (with finite accumulation points) nor chaotic solutions were obtained.

The investigation in §5 was undertaken in connection with the experimental work of Altman (1985). It is hoped that his results, together with a comparison with the present theory, will be published soon.

The joint limit $N \uparrow \infty$ and $d_\nu \downarrow 0$ yields the Lagrangian density for a continuously stratified fluid (cf. Miles 1986, §6). Unfortunately, the coefficients in this formal model contain divergent integrals in consequence of the singularity at the critical layer. The resolution of this difficulty appears to require a rescaling in the neighbourhood of the critical layer and perhaps also the introduction of diffusive interior layers; see Stewartson (1981) and references cited there.

† The basic flow in these experiments is induced by tilting the wave tank. This flow is accelerated while the tank is tilted, and the present formulation is applicable only after the tank has been restored to a horizontal position and the basic flow is approximately uniform. The present formulation can be generalized to accelerated flow, but the transition to K–H instability then corresponds to a turning point of the linear differential equation, and weak nonlinearity is likely to be dominated by acceleration.

2. Lagrangian for layered fluid

The horizontally averaged Lagrangian for an N-layered fluid may be placed in the form

$$\mathscr{L} = \sum_{\nu=1}^{N} \rho_\nu L_1(\boldsymbol{q}_\nu, \dot{\boldsymbol{q}}_\nu, \boldsymbol{q}_{\nu-1}, \dot{\boldsymbol{q}}_{\nu-1}; d_\nu, \boldsymbol{U}_\nu), \tag{2.1}$$

where: ρ_ν, d_ν and $\boldsymbol{U}_\nu$ are the density, undisturbed depth and ambient velocity (horizontal) for the νth layer; $\boldsymbol{q}_\nu \equiv \{q_n^\nu(t)\}$ is the set of generalized coordinates defined by the Fourier expansion of the displacement of the νth interface ($\nu = 0, \ldots, N$)

$$\eta_\nu(\boldsymbol{x}, t) = q_n^\nu(t)\, \mathrm{e}^{\mathrm{i}\boldsymbol{k}\cdot n\boldsymbol{x}}; \tag{2.2}$$

the $\exp(\mathrm{i}\boldsymbol{k}_n\cdot\boldsymbol{x})$ form a complete set of normal modes in the horizontal and occur in complex-conjugate pairs, $\boldsymbol{k}_{\bar{n}} \equiv -\boldsymbol{k}_n$ and $q_{\bar{n}} \equiv q_n^*$, and, here and subsequently except as noted, the repeated index n is summed over the complete spectrum†; $\rho L_1(\boldsymbol{q}_+, \dot{\boldsymbol{q}}_+, \boldsymbol{q}_-, \dot{\boldsymbol{q}}_-; d, \boldsymbol{U})$ is the corresponding Lagrangian for a single layer of fluid for which $\boldsymbol{q}_\pm$ is the generalized coordinate of the upper/lower surface. L_1 may be obtained from the corresponding result for $\boldsymbol{U} = 0$ through the Galilean transformation

$$\dot{q}_n^\pm(t) \to \left(\frac{\mathrm{d}}{\mathrm{d}t} + \mathrm{i}\boldsymbol{k}_n\cdot\boldsymbol{U}\right) q_n^\pm(t) \equiv p_n^\pm(t). \tag{2.3}$$

The end result is [Miles 1986, equations (3.10), (5.2)–(5.4)]

$$\begin{aligned} 2L_1 = {} & \delta_{mn}[a_n(p_m^+ p_n^+ - 2S_n p_m^+ p_n^- + p_m^- p_n^-) - g(q_m^+ q_n^+ - q_m^- q_n^-)] \\ & + \delta_{lmn}\{q_l^+ p_m^+ p_n^+ - q_l^- p_m^- p_n^- + a_m a_n(\boldsymbol{k}_m\cdot\boldsymbol{k}_n)[q_l^+(p_m^+ - S_m p_m^-)(p_n^+ - S_n p_n^-) \\ & - q_l^-(p_m^- - S_m p_m^+)(p_n^- - S_n p_n^+)]\} + \delta_{mn} a_n(r_m^+ r_n^+ + 2S_n r_m^+ r_n^- + r_m^- r_n^-) \\ & + \tfrac{1}{2}\delta_{jlmn}\{k_m^2 a_m[q_j^+ q_l^+(S_n p_m^+ p_n^- - S_m p_m^- p_n^+) + q_j^- q_l^-(S_n p_m^- p_n^+ - S_m p_m^+ p_n^-)] \\ & + (a_m + a_n)(\boldsymbol{k}_m\cdot\boldsymbol{k}_n)[q_j^+ q_l^+(p_m^+ - S_m p_m^-) p_n^+ + q_j^- q_l^-(p_m^- - S_m p_m^+) p_n^-]\}, \end{aligned} \tag{2.4}$$

where $$\delta_{mn} = \begin{matrix} 1 \\ 0 \end{matrix} \quad \text{for } \boldsymbol{k}_m + \boldsymbol{k}_n \begin{matrix} = \\ \neq \end{matrix} 0, \quad \delta_{lmn} = \begin{matrix} 1 \\ 0 \end{matrix} \quad \text{for } \boldsymbol{k}_l + \boldsymbol{k}_m + \boldsymbol{k}_n \begin{matrix} = \\ \neq \end{matrix} 0 \tag{2.5a, b}$$

and similarly for δ_{jlmn},

$$a_n = (k_n \tanh k_n d)^{-1}, \quad k_n = |\boldsymbol{k}_n|, \quad S_n = \operatorname{sech} k_n d, \tag{2.6a, b, c}$$

$$r_n^\pm = -\delta_{lm\bar{n}} a_m \boldsymbol{k}_m\cdot\boldsymbol{k}_n q_l^\pm(p_m^\pm - S_m p_m^\mp) \quad (n \text{ not summed}). \tag{2.7}$$

The configuration of a single interface with rigid, plane upper and lower boundaries is obtained by setting $N = 2$, $\boldsymbol{q}_0 = \boldsymbol{q}_2 = 0$, $\boldsymbol{q}_1 \equiv \boldsymbol{q}$, $\rho_{1,2} \equiv \rho_\mp$, $d_{1,2} \equiv d_\mp$ and $U_{1,2} \equiv U_\pm$ in (2.1), which then reduces to

$$\mathscr{L} = \rho_+ L_1(0, 0, \boldsymbol{q}, \dot{\boldsymbol{q}}; d_+, U_+) + \rho_- L_1(\boldsymbol{q}, \dot{\boldsymbol{q}}, 0, 0; d_-, U_-). \tag{2.8}$$

Substituting (2.4) into (2.8), truncating at $n = \pm 2$, which is consistent with the quartic approximation to L_1 on the hypothesis that $kq_n = O(k^n q_1^n)$, and neglecting $O(k^6 q_1^6)$, we obtain

$$\begin{aligned} \mathscr{L} = {} & \rho_\pm\{a_1 p_1 p_1^* + a_2 p_2 p_2^* \pm g(q_1 q_1^* + q_2 q_2^*) \\ & \mp \tfrac{1}{2}(1 + k_1^2 a_1^2)(q_2^* p_1^2 + q_2 p_1^{*2}) \mp (1 - a_1 a_2 \boldsymbol{k}_1\cdot\boldsymbol{k}_2)(q_1 p_1 p_2^* + q_1^* p_1^* p_2) \\ & + \tfrac{1}{2} a_1 k_1^2(q_1^2 p_1^{*2} + q_1^{*2} p_1^2) + [a_1^2 a_2(\boldsymbol{k}_1\cdot\boldsymbol{k}_2)^2 - 2a_1 k_1^2] q_1 q_1^* p_1 p_1^*\}_\pm, \end{aligned} \tag{2.9}$$

† The index n is an abbreviation for a couplet of indices, say (n_x, n_y), for three-dimensional problems, in which $\boldsymbol{x} \equiv (x, y)$ and $\boldsymbol{k}_n \equiv (n_x k_x, n_y k_y)$. Only two-dimensional problems, in which $\boldsymbol{k}_n \equiv (nk, 0)$, are considered below.

wherein the $\pm$ subscript now refers to the upper/lower layer, $d = d_\pm$ and $U = U_\pm$ in the evaluation of a_n and p_n in the upper/lower layer, and summation over the vertically ordered, alternative signs and subscripts is implicit.

3. Interfacial progressive waves

Considering a progressive wave of permanent form for which the first approximation has the form $\eta = A\cos k(x-ct)$ with $kA \ll 1$, we posit

$$\boldsymbol{k}_n = (nk, 0), \quad q_n = k^{-1}A_n\,\mathrm{e}^{-\mathrm{i}nkct} \quad (n = \pm 1, \pm 2), \tag{3.1a, b}$$

where A_1 and A_2 are dimensionless amplitudes that (in this section) may be taken to be real without loss of generality. Substituting (3.1) into (2.3) and (2.9), we obtain

$$\begin{aligned}\mathscr{L} = \rho_\pm\, k^{-1}\{&T_\pm^{-1}(U_\pm - c)^2[A_1^2 + (1+T_\pm^2)A_2^2] \pm (g/k)(A_1^2 + A_2^2)\\ &\pm (3T_\pm^{-2}-1)(U_\pm - c)^2 A_1^2 A_2 - (2T_\pm^{-1} - T_\pm^{-3})(U_\pm - c)^2 A_1^4\},\end{aligned} \tag{3.2}$$

wherein the conventions of (2.9) apply and

$$T_\pm \equiv \tanh kd_\pm. \tag{3.3}$$

Requiring $\mathscr{L}$ to be stationary with respect to independent variations of A_1 and A_2, solving the resulting algebraic equations for A_2 and c, neglecting $O(A_1^4)$, and invoking $A_1 \equiv \frac{1}{2}kA$, we obtain

$$\frac{A_2}{A_1^2} = \frac{1}{2}\left[\frac{\rho_-(3T_-^{-2}-1)(U_- - c)^2 - \rho_+(3T_+^{-2}-1)(U_+ - c)^2}{\rho_- T_-(U_- - c)^2 + \rho_+ T_+(U_+ - c)^2}\right] \equiv B, \tag{3.4}$$

$$c = \overline{U} \pm [c_1^2(1 + \tfrac{1}{2}Ck^2A^2) + \overline{U}^2 - \overline{U^2}]^{\frac{1}{2}}, \tag{3.5}$$

wherein

$$c_1^2 = \frac{(\rho_- - \rho_+)(g/k)}{\rho_+ T_+^{-1} + \rho_- T_-^{-1}}, \quad \overline{U^n} = \frac{\rho_+ T_+^{-1} U_+^n + \rho_- T_-^{-1} U_-^n}{\rho_+ T_+^{-1} + \rho_- T_-^{-1}} \quad (n = 1, 2), \tag{3.6a, b}$$

$$C = \frac{\rho_+(2T_+^{-1} - T_+^{-3})(U_+ - c)^2 + \rho_-(2T_-^{-1} - T_-^{-3})(U_- - c)^2 + B^2[\rho_+ T_+(U_+ - c)^2 + \rho_- T_-(U_- - c)^2]}{\rho_+ T_+^{-1}(U_+ - c)^2 + \rho_- T_-^{-1}(U_- - c)^2} \tag{3.7}$$

The corresponding interfacial displacement, obtained by combining (2.2) and (3.1), is

$$\eta = A\cos k(x-ct) + \tfrac{1}{2}kA^2 B\cos 2k(x-ct). \tag{3.8}$$

The first approximation to c is obtained by neglecting k^2A^2 in (3.5). The second approximation is obtained by substituting this first approximation into (3.4) and (3.7) and then substituting the resulting approximation to C into (3.5).

Kelvin–Helmholtz instability occurs for $|U_+ - U_-| > U_*$ (so that the wave speeds given by (3.5) are complex), where

$$U_*^2 = \frac{(\rho_+ T_- + \rho_- T_+)(\rho_- - \rho_+)g}{\rho_+ \rho_- k}(1 + \tfrac{1}{2}Ck^2A^2). \tag{3.9}$$

The values of B and C for $|U_+ - U_-| = U_*$ (which implies $c = \overline{U}$) are

$$B_* = \frac{1}{2}\left[\frac{\rho_+(3-T_-^2) - \rho_-(3-T_+^2)}{\rho_+ T_-^3 + \rho_- T_+^3}\right], \quad C_* = 2 - \left(\frac{\rho_+ T_-^{-1} + \rho_+ T_+^{-1}}{\rho_+ T_- + \rho_- T_+}\right) + B_*^2\left(\frac{\rho_+ T_-^3 + \rho_- T_+^3}{\rho_+ T_- + \rho_- T_+}\right). \tag{3.10a, b}$$

We remark that $\mathrm{d}U_*^2/\mathrm{d}A^2 \gtrless 0$ for $C_* \gtrless 0$ and that the corresponding pitchfork bifurcation at $\overline{U^2} - \overline{U}^2 = c_1^2$ is supercritical/subcritical (normal/inverted). C_* is not

generally positive-definite; e.g. $C_* = 2 - T^{-2}$ for $\rho_+ \approx \rho_-$ (the Boussinesq approximation) and $d_+ = d_- = d$, which implies $C_* < 0$ for $kd < 0.881$. If $kh_\pm \gg 1$, $C_* = 1 + B_*^2$ is positive-definite; however, this does not hold if surface tension is admitted, in which case (see Appendix A) C_* not only may be negative but also may be singular (along with B_*) in consequence of resonance between a gravity-capillary wave and its second harmonic.

Letting $kh_\pm \uparrow \infty$ ($T_\pm \uparrow 1$) in (3.4)–(3.8), we recover the results of Maslowe & Kelly (1970), Saffman & Yuen (1982) and, after incorporating surface tension (see Appendix A) and correcting a typographical error in their equation (3.26), Nayfeh & Saric (1972).

Linear damping may be modelled in the present problem by introducing the dissipation function

$$\mathscr{D} = D\rho_\pm \varkappa_\pm (p_1 p_1^*)_\pm \tag{3.11a}$$

$$= D(\rho_+ \varkappa_+ + \rho_- \varkappa_-)[\dot{q}_1 \dot{q}_1^* + \mathrm{i}k\overline{U}(q_1 \dot{q}_1^* - q_1^* \dot{q}_1) + k^2 \overline{U^2} q_1 q_1^*], \tag{3.11b}$$

where D is a positive damping constant that is assumed to have the same value in the two layers (if this assumption is not satisfied the weighted averages of $U_\pm$ and $U_\pm^2$ will differ from $\overline{U}$ and $\overline{U^2}$ in (3.11*b*)). The equation of motion for q_1 then becomes

$$\frac{\mathrm{d}}{\mathrm{d}t}\frac{\partial \mathscr{L}}{\partial \dot{q}_1^*} - \frac{\partial \mathscr{L}}{\partial q_1^*} + \frac{\partial \mathscr{D}}{\partial \dot{q}_1^*} = 0, \tag{3.12}$$

which implies the introduction of $-\mathrm{i}(D/2k)$ on the right-hand side of (3.5) and of $-(D/2k)^2$ in the radical therein.

4. Kelvin–Helmholtz instability

We now examine the parametric neighbourhood of $|U_+ - U_-| = U_*$, positing

$$q_n(t) = \epsilon^{|n|} k^{-1} A_n(\tau)\, \mathrm{e}^{-\mathrm{i}nk\overline{U}t} \quad (n = \pm 1, \pm 2), \quad \tau = \epsilon |C_*|^{\frac{1}{2}} k c_1 t \tag{4.1a, b}$$

on the hypotheses that A_n, τ and

$$\beta \equiv \frac{c_1^2 + \overline{U}^2 - \overline{U^2}}{\epsilon^2 |C_*| c_1^2} \tag{4.2}$$

are $O(1)$ as $\epsilon \downarrow 0$. The introduction of the scaling factor $|C_*|$, as given by (3.10*b*), in (4.1*b*) and (4.2) simplifies the subsequent development (the problem is linear in the present approximation if $C_* = 0$). Note that A_n is rescaled *vis-à-vis* A_n in §3 and now is (in general) complex.

Substituting (4.1) into (2.3) and (2.9) and invoking (3.6*a*, *b*) and (4.2), we obtain [cf. (3.2)]

$$\mathscr{L} = \rho_\pm k^{-1} \epsilon^4 c_1^2 \Big\{ |C_*| T_\pm^{-1} (\dot{A}_1 A_1^* - \beta A_1 A_1^*) + T_\pm \Big(\frac{U_\pm - \overline{U}}{c_1}\Big)^2 A_2 A_2^*$$

$$\pm \tfrac{1}{2}(3T_\pm^{-2} - 1)\Big(\frac{U_\pm - \overline{U}}{c_1}\Big)^2 (A_1^2 A_2^* + A_1^{*2} A_2) - (2T_\pm^{-1} - T_\pm^{-3})\Big(\frac{U_\pm - \overline{U}}{c_1}\Big)^2 A_1^2 A_1^{*2} \Big\}, \tag{4.3}$$

wherein $\dot{A}_1 \equiv \mathrm{d}A_1/\mathrm{d}\tau$, and summation over the vertically ordered, alternative signs and an error factor of $1 + O(\epsilon^2)$ are implicit. Invoking $\delta \mathscr{L}/\delta A_2^* = 0$, we obtain [cf. (3.4)]

$$\frac{A_2}{A_1^2} = B|_{c=\overline{U}} = B_*, \tag{4.4}$$

where B_* is given by (3.10a). Using (4.4) to eliminate A_2 and A_2^* from (4.3), invoking (3.6a, b) and (3.7) for C with $c = U$ therein, which then reduces to C_*, and introducing the real variables $R(\tau)$ and $\theta(\tau)$ through the transformation

$$A_1 = R\,\mathrm{e}^{\mathrm{i}\theta}, \tag{4.5}$$

we obtain (after some reduction)

$$\mathscr{L} = \epsilon^4|C_*|(\rho_- - \rho_+)\,gk^{-2}(\dot{R}^2 + R^2\dot{\theta}^2 - \beta R^2 - \gamma R^4), \tag{4.6}$$

where $\gamma \equiv \operatorname{sgn} C_*$ ($\gamma = C_*$ if $|C_*|$ is omitted in (4.1b), (4.2) and (4.6)). We note that (4.5), in conjunction with (4.1a) and (4.4), implies

$$\tfrac{1}{2}k\eta = \epsilon R(\tau)\cos\phi + \epsilon^2 B_*\,R^2(\tau)\cos 2\phi, \quad \phi = k(x - \overline{U}t) + \theta(\tau). \tag{4.7a, b}$$

Invoking $\delta\mathscr{L}/\delta R = 0$ and $\delta\mathscr{L}/\delta\theta = 0$ and introducing $\omega \equiv \dot{\theta}$, we obtain

$$\ddot{R} + \beta R + 2\gamma R^3 - R\omega^2 = 0, \quad R^2\dot{\omega} + 2R\dot{R}\omega = 0, \quad \dot{\theta} = \omega, \tag{4.8a, b, c}$$

which admit the first integrals

$$\dot{R}^2 + \beta R^2 + \gamma R^4 + M^2R^{-2} = E, \quad R^2\omega = M \tag{4.9a, b}$$

(which also may be inferred directly from the invariance of $\mathscr{L}$ under translations of τ and θ). The parameters M and E, which are determined by the initial conditions, are analogues of angular momentum and energy for a particle in a central force field with the potential $\frac{1}{2}(\beta R^2 + \gamma R^4)$.

The progressive wave of §3 corresponds to a fixed point of (4.8) in an $(R, \dot{R}, \omega)$-space (the coordinate θ being ignorable) at which

$$\omega = \frac{\overline{U} - c}{\epsilon|C_*|^{\frac{1}{2}}c_1}, \quad \beta + 2\gamma R^2 - \omega^2 = \dot{R} = 0. \tag{4.10a, b}$$

[The present formulation for this progressive wave is valid only for ω and $\beta = O(1)$ but may be rendered uniformly valid for all real c simply by replacing B_* and C_* by B and C, as given by (3.4) and (3.7).] The stability of this fixed point with respect to small perturbations of the form $\exp(\lambda\tau)$ is determined by the characteristic equation

$$\begin{vmatrix} \lambda^2 + \beta + 6\gamma R^2 - \omega^2 & -2R\omega \\ 2R\omega\lambda & R^2\lambda \end{vmatrix} = R^2\lambda(\lambda^2 + \beta + 6\gamma R^2 + 3\omega^2) = 0. \tag{4.11}$$

It follows from (4.10b) and (4.11) that the fixed point is stable for all $kA = O(\epsilon)$ if $C_* > 0$, but if $C_* < 0$ it is stable if and only if

$$k^2A^2 < \tfrac{4}{3}|C_*|^{-1}\left[1 - \left(\frac{\overline{U^2} - \overline{U}^2}{c_1^2}\right)\right] = O(\epsilon). \tag{4.12}$$

The differential equations (4.8) are equivalent to Weissman's (1979) equations (3.02) and (3.03). Weissman takes $kh_\pm = \infty$ but includes capillarity, so that his counterpart of C_* may have either sign (see Appendix A). He obtains the first integral (4.9a) in the special case $M = 0$, for which A_1 may be taken to be real. The fixed points of (4.8a) in an $(A_1, \dot{A}_1)$-plane then are at $A_1 = \dot{A}_1 = 0$, which is a centre/saddle point (stable/unstable) for $\beta \gtrless 0$; $A_1 = \pm(-\beta/2\gamma)^{\frac{1}{2}}$, $\dot{A}_1 = 0$, which exist if and only if β and C_* have opposite signs and are centres/saddle points for $C_* \gtrless 0$. The four possible forms of the trajectories (corresponding to the four possible sign pairings of β and γ) are sketched in Weissman's figure 2. This special case also has been discussed by Drazin (1970) and Nayfeh & Saric (1972). Drazin imposes the Boussinesq

approximation [neglecting $(\rho_- - \rho_+)/(\rho_- + \rho_+)$ except in the buoyancy term], which eliminates the possibility of second-harmonic resonance. After allowing for this difference and correcting what appears to be a typographical error ($1+4\alpha^2$ should be $4+\alpha^2$), I find that his equation (41) is equivalent to (4.9a) above with $M = 0$ therein. Nayfeh & Saric obtain results similar to those of Weissman for those two cases for which β and γ have opposite signs.

The general solution of (4.9) may be expressed in terms of elliptic integrals through the transformation $Z = R^2$, which yields

$$\tfrac{1}{4}\dot{Z}^2 = -M^2 + EZ - \beta Z^2 - \gamma Z^3 \equiv F(Z). \tag{4.13}$$

The character of these solutions depends on the disposition of the zeros of $F(Z)$.

(i) If $\beta > 0$ and $\gamma = 1$, $F(Z)$ has two and only two positive zeros, and closed trajectories in the $(Z, \dot{Z})$-plane exist, if and only if $E > 0$ and

$$F(Z_c) > 0, \quad Z_c = \tfrac{1}{3}[(\beta^2 + 3E)^{\frac{1}{2}} - \beta], \tag{4.14a, b}$$

where Z_c is the positive zero of F'. The modulational period (on the τ-scale) then is given by

$$T = \int_b^a \frac{\mathrm{d}Z}{[(a-Z)(Z-b)(Z-c)]^{\frac{1}{2}}} = \frac{2}{(a-c)^{\frac{1}{2}}} K\left[\left(\frac{a-b}{a-c}\right)^{\frac{1}{2}}\right], \tag{4.15}$$

where $a > b > 0 > c$ are the zeros of $F(Z)$, and K is a complete elliptic integral of the first kind.

(ii) If $\beta < 0$ and $\gamma = 1$, F has two and only two positive zeros, and closed trajectories exist, for all real E if and only if

$$F(Z_c) > 0, \quad Z_c = \tfrac{1}{3}[|\beta| + (\beta^2 + 3E)^{\frac{1}{2}}]. \tag{4.16a, b}$$

The corresponding period is given by (4.15).

(iii) If $\beta > 0$ and $\gamma = -1$, $F(Z)$ has three positive zeros, and both closed and open trajectories exist, if $E > 0$ and

$$F(Z_c^-) > 0, \quad F(Z_c^+) < 0, \quad Z_c^{\pm} = \tfrac{1}{3}[\beta \pm (\beta^2 - 3E)^{\frac{1}{2}}]. \tag{4.17a, b, c}$$

The corresponding period is given by

$$T = \int_c^b \frac{\mathrm{d}Z}{[(a-Z)(b-Z)(Z-c)]^{\frac{1}{2}}} = \frac{2}{(a-c)^{\frac{1}{2}}} K\left[\left(\frac{b-c}{a-c}\right)^{\frac{1}{2}}\right], \tag{4.18}$$

where $a > b > c > 0$ are the zeros of $F(Z)$. Otherwise, F has only one positive zero, and only divergent trajectories exist.

(iv) If $\beta < 0$ and $\gamma = -1$, F has one and only one positive zero, and only divergent trajectories exist.

We emphasize that, although the closed trajectories in the $(Z, \dot{Z})$-plane correspond to periodic $R(\tau)$, the period of R generally differs from that of θ mod 2π, as determined from (4.9b) and (4.8c), in consequence of which the trajectories in the (R, θ)-plane are closed only for exceptional initial conditions.†

Weak damping may be incorporated as in the last paragraph in §3 and leads to the equations of motion (polar coordinates are no longer advantageous)

$$\ddot{A}_1 + 2\delta\dot{A}_1 + (\beta + 2\gamma|A_1|^2)A_1 = 0 \tag{4.19}$$

† It follows from Bertrand's theorem (Goldstein 1980, §3.6) that closed R versus θ orbits for a particle in a central force field exist for all initial conditions only for either linear (Hooke's law) or inverse-square forces.

and its complex-conjugate, (4.19)*, where

$$\delta = (2\epsilon|C_*|^{\frac{1}{2}}kc_1)^{-1}D \tag{4.20}$$

is a dimensionless damping parameter that must be $O(1)$ for the damping to be *weak* in the present context. The fixed points of (4.19) are at either $A_1 = \dot{A}_1 = 0$ or $|A_1| = (-\beta/2\gamma)^{\frac{1}{2}}$, $\dot{A}_1 = 0$, as in the undamped case with $M = 0$. [It can be deduced from (4.19) and (4.19)* that $\dot{M} = -2\delta M$, so that Weissman's assumption that $M = 0$ is replaced by the deduction that any initial value of M decays like $\exp(-2\delta\tau)$.] The stability of these fixed points with respect to small perturbations of A_1 and A_1^* of the form $\exp(\lambda\tau)$ is determined by

$$\begin{vmatrix} \lambda^2+2\delta\lambda+\beta+4\gamma|A_1|^2 & 2\gamma A_1^2 \\ 2\gamma A_1^{*2} & \lambda^2+2\delta\lambda+\beta+4\gamma|A_1|^2 \end{vmatrix}$$
$$= (\lambda^2+2\delta\lambda+\beta+2\gamma|A_1|^2)(\lambda^2+2\delta\lambda+\beta+6\gamma|A_1|^2). \tag{4.22}$$

It follows that the fixed point at $A_1 = 0$ is stable/unstable for $\beta \gtrless 0$, whilst that at $|A_1| = (-\beta/2\gamma)^{\frac{1}{2}}$ is stable/unstable for $\beta \lesssim 0$. In brief, the locations of the fixed points and the stability criteria for weak damping remain as in Weissman's special case ($M = 0$) of the undamped problem, whilst the centres/saddle points become stable/unstable spiral singularities.

5. Resonant forcing

We consider next the wave motion forced by flow over the sinusoidal bottom

$$\eta_0 = a\cos kx, \tag{5.1}$$

on the assumption that $c_1^2 \doteq \overline{U^2}$ ($c_1^2 = \overline{U^2}$ implies resonance between the sinusoidal bottom and a standing interfacial wave). The displacement (5.1) of the lower boundary implies $\boldsymbol{q}_0 = \{q_1^0, q_{\bar{1}}^0\} = \{\frac{1}{2}a, \frac{1}{2}a\}$ in place of $\boldsymbol{q}_0 = 0$ in (2.8), which, in turn, implies the addition of

$$-[\rho a_1 S_1(\tfrac{1}{2}ikUa)(p_1^*-p_1)]_-$$

to the Lagrangian (2.9) (it also implies the addition of higher-order terms, which prove to be negligible, and of the constant $\frac{1}{4}ga^2$, which has no dynamical significance). Positing $\boldsymbol{k}_n = (nk, 0)$ and

$$q_n(t) = \epsilon^{|n|}k^{-1}A_n(\tau) \quad (n = \pm 1, \pm 2), \quad \tau = \epsilon|C_0|^{\frac{1}{2}}kc_1 t, \tag{5.2a, b}$$

in this augmented form of (2.9), introducing

$$\alpha \equiv \frac{\overline{U}}{\epsilon|C_0|^{\frac{1}{2}}c_1}, \quad \beta \equiv \frac{c_1^2-\overline{U^2}}{\epsilon^2|C_0|c_1^2}, \quad \gamma \equiv \operatorname{sgn} C_0, \tag{5.3a, b, c}$$

[note that β(5.3b) differs from β(4.2)], where c_1^2, $\overline{U}$, $\overline{U^2}$ and C_0 are given by (3.6) and (3.7) with $c = 0$ therein, proceeding as in §4 on the hypothesis that α and $\beta = O(1)$,† and choosing

$$\epsilon^3 = \frac{\rho_-(U_-/c_1)^2 ka}{2|C_0|(\rho_+ T_+^{-1}+\rho_- T_-^{-1})\sinh kd_-}, \tag{5.4}$$

† It can be shown, by a parallel investigation of the appropriately rescaled problem, that the following analysis is uniformly valid for large α; however, the most interesting results are obtained for $\alpha = O(1)$.

we obtain

$$\mathscr{L} = \epsilon^4|C_0|(\rho_- - \rho_+)\,gk^{-2}[(\dot{A}_1 + \mathrm{i}\alpha A_1)(\dot{A}_1^* - \mathrm{i}\alpha A_1^*) - (\alpha^2+\beta)\,A_1 A_1^* - \gamma A_1^2 A_1^{*2} - (A_1 + A_1^*)]. \quad (5.5)$$

Invoking $\delta\mathscr{L}/\delta A_1^* = 0$ and $\delta\mathscr{L}/\delta A_1 = 0$, we obtain

$$\ddot{A}_1 + 2\mathrm{i}\alpha\dot{A}_1 + (\beta + 2\gamma|A_1|^2)\,A_1 = -1 \quad (5.6)$$

and its complex-conjugate, (5.6)*. It follows from (5.6) and (5.6)*, or directly from the invariance of $\mathscr{L}$ (5.5) under a translation of τ, that

$$|\dot{A}_1|^2 + \beta|A_1|^2 + \gamma|A_1|^4 + A_1 + A_1^* \equiv H \quad (5.7)$$

is a constant of the motion, which may be identified as a dimensionless Hamiltonian (Appendix B). It follows from (5.7) that the forced motion is bounded for $\gamma = 1$ but may diverge for $\gamma = -1$.

Weak damping may be incorporated as in the last paragraphs in §§3 and 4 and implies the introduction of $2\delta(\dot{A}_1 + \mathrm{i}\alpha A_1)$ on the left-hand sides of (5.6) and (5.6)* to obtain [cf. (4.19)]

$$\ddot{A}_1 + 2(\delta + \mathrm{i}\alpha)\,\dot{A}_1 + (\beta + 2\mathrm{i}\alpha\delta + 2\gamma|A_1|^2)\,A_1 = -1 \quad (5.8)$$

and its complex-conjugate, (5.8)*, where δ is given by (4.20) with C_* replaced by C_0 therein.

The fixed points of (5.8) and (5.8)* in the $X, Y, \dot{X}, \dot{Y} (X + \mathrm{i}Y \equiv A_1)$ phase space are determined by $\dot{X} = \dot{Y} = 0$ and

$$[\mu^2 + (\beta + 2\gamma R^2)^2]\,R^2 = 1 \ (\mu \equiv 2|\alpha|\delta), \quad \tan\theta = \frac{-2\alpha\delta}{\beta + 2\gamma R^2}, \quad A_1 = R\,\mathrm{e}^{\mathrm{i}\theta} \quad (5.9a, b, c)$$

and correspond to a stationary wave. The resonance curve (locus of fixed points) determined by (5.9a) for $\gamma = 1$ is plotted in figure 1. It has a maximum of $R = 1/\mu$ at $\beta = -2\gamma/\mu^2$ and is triple-valued for $\beta_c^u < \beta < \beta_c^\ell$, where β_c^u and β_c^ℓ are the upper and lower turning points determined by (see figure 2)

$$\beta_c = -2\gamma(R_c^2 + \tfrac{1}{8}R_c^{-4}), \quad 16R_c^6(1 - \mu^2 R_c^2) = 1 \quad (\mu < \mu_c = 3^{\frac{1}{2}} \times 4^{-\frac{1}{3}} = 1.091). \quad (5.10a, b)$$

The upper and lower turning points coalesce for $\mu = \mu_c$, and the resonance curve is single-valued for $\mu > \mu_c$. The resonance curve for $\gamma = -1$ is obtained from that for $\gamma = +1$ through the reflection $\beta \to -\beta$, but the division of this curve into stable and unstable segments (see below) is not invariant under this transformation.

The stability of a particular fixed point with respect to small perturbations of A_1 and A_1^* (or, equivalently, X and Y) of the form $\exp(\lambda\tau)$ is determined by

$$\begin{vmatrix} \lambda^2 + 2(\delta + \mathrm{i}\alpha)\,\lambda + \hat{\beta} + 2\mathrm{i}\alpha\delta & 2\gamma A_1^2 \\ 2\gamma A_1^{*2} & \lambda^2 + 2(\delta - \mathrm{i}\alpha)\,\lambda + \hat{\beta} - 2\mathrm{i}\alpha\delta \end{vmatrix}$$

$$= \lambda^4 + 4\delta\lambda^3 + 2(2\alpha^2 + 2\delta^2 + \hat{\beta})\,\lambda^2 + 4\delta(2\alpha^2 + \hat{\beta})\,\lambda + 4\alpha^2\delta^2 + \hat{\beta}^2 - 4R^4 = 0$$

$$(\hat{\beta} \equiv \beta + 4\gamma R^2). \quad (5.11)$$

The necessary and sufficient conditions for stability (which requires that no root of (5.11) have a positive real part) are

$$\hat{\beta}^2 \geqslant 4(R^4 - \alpha^2\delta^2), \quad 2\alpha^2 + \hat{\beta} \geqslant 0, \quad \alpha^2 + \hat{\beta} + \frac{R^4}{\alpha^2 + \delta^2} \geqslant 0. \quad (5.12a, b, c)$$

It can be shown that all of (5.12a, b, c) are satisfied on the upper branch ($\beta > \beta_c^u$) of the resonance curve for $\gamma = 1$ and on the lower branch ($\beta > \beta_c^\ell$) for $\gamma = -1$, which

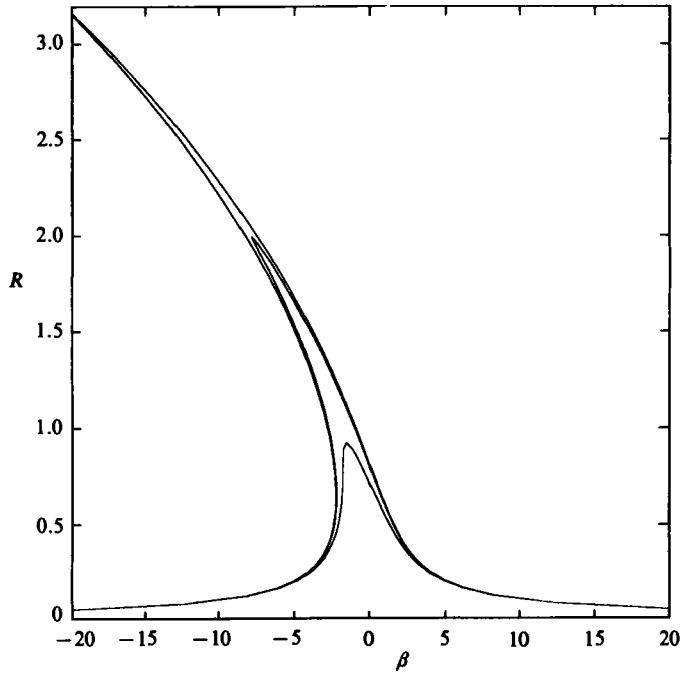

FIGURE 1. The resonance curves determined by (5.9*a*) for $\gamma = 1$ and $\mu^2 \equiv 4\alpha^2\delta^2 = \frac{1}{10}, \frac{1}{4}$ and 1.191 (upper/middle/lower curve). The turning points coalesce for $\mu = 1.191$, and the resonance curves for $\mu > 1.191$ are single valued. The middle branch is unstable; in addition, that segment of the lower branch to the left of the Hopf-bifurcation point (see text) is unstable. The resonance curves for $\gamma = -1$ are obtained through those for $\gamma = 1$ through the reflection $\beta \to -\beta$, but the Hopf bifurcations (of which there may be 0, 1, 2 or 3) then are on the upper branch (see text).

therefore are stable (or, more precisely, comprise only stable fixed points). Equality in (5.12*a*) is attained at the turning points, and the middle branch of the resonance curve, which lies between these turning points and violates (5.12*a*), is unstable for either $\gamma = 1$ or $\gamma = -1$. Equality in (5.12*c*), together with the satisfaction of (5.12*a*, *b*), corresponds to a Hopf bifurcation. Eliminating β between this equality and (5.9*a*) and invoking the inequality (5.12*b*), we obtain

$$[(\alpha^2+\delta^2)^{\frac{1}{2}}+\gamma(\alpha^2+\delta^2)^{-\frac{1}{2}}R^2]^2 = \delta^2 \pm (R^{-2}-4\alpha^2\delta^2)^{\frac{1}{2}}, \tag{5.13a}$$

$$R^2 \equiv R_{\mathrm{H}}^2 \leqslant |\alpha|(\alpha^2+\delta^2)^{\frac{1}{2}}, \tag{5.13b}$$

where the $\pm$ sign in (5.13*a*) corresponds to the left/right (with respect to the peak) side of the resonance curve. The corresponding values of β, if any, are given by

$$\beta_{\mathrm{H}} = -\alpha^2 - 4\gamma R_{\mathrm{H}}^2 - (\alpha^2+\delta^2)^{-1}R_{\mathrm{H}}^4. \tag{5.13c}$$

The parametric evolution of the Hopf bifurcations may be elucidated by examining the intersections of the left- and right-hand sides of (5.13*a*) in $0 \leqslant R_{\mathrm{H}}^2 \leqslant |\alpha|(\alpha^2+\delta^2)^{\frac{1}{2}}$. Considering $\gamma = 1$ first, we find that there is one and only one such intersection if and only if $|\alpha| > \alpha_+$, where α_+ is determined by equality in (5.13*b*), which, in conjunction with (5.13*a*), implies (see figure 3)

$$8\alpha^3(\alpha^2+\delta^2)[\alpha+(\alpha^2+\delta^2)^{\frac{1}{2}}] = 1 \quad (\alpha = \alpha_+). \tag{5.14}$$

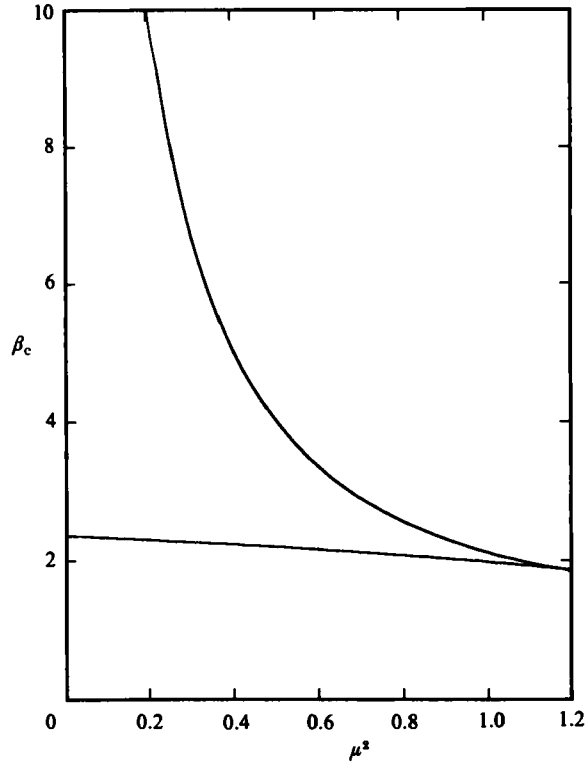

FIGURE 2. The turning points determined by (5.10). The two turning points coalesce for $\mu^2 = 1.191$ and disappear for $\mu^2 > 1.191$.

Approximations for small and large δ are

$$\alpha_+ = 0.630[1-0.525\delta^2+O(\delta^4)] \quad (\delta\downarrow 0), \quad \alpha_+ \sim \tfrac{1}{2}\delta^{-1}-\tfrac{1}{12}\delta^{-3}+O(\delta^{-5}) \quad (\delta\uparrow\infty). \tag{5.15a, b}$$

The entire lower branch of the resonance curve is unstable if $|\alpha| < \alpha_+$. The Hopf bifurcation emerges from the lower turning point, $\beta = \beta_c'$, at $|\alpha| = \alpha_+$, and the segment $\beta_H < \beta < \beta_c'$ of the lower branch is stable ($\beta < \beta_H$ is unstable) for $\alpha_+ < |\alpha| < \mu_c/2\delta$. The resonance curve is single-valued and stable/unstable for $\beta \gtrless \beta_H$ if $|\alpha| > \mu_c/2\delta$ (it can be shown that $\alpha_+ < \mu_c/2\delta$; see figure 3).

The evolution of the Hopf bifurcations for $\gamma = -1$ is more complicated than for $\gamma = 1$, and we consider only $\delta \ll 1$ (the most interesting case) in detail. There then may be 0, 1, 2 or 3 intersections of the right-hand side of (5.13a) with the parabola represented by the left-hand side thereof within the range $0 < R_H^2 \leqslant |\alpha|(\alpha^2+\delta^2)^{\frac{1}{2}} < \alpha^2+\delta^2$. There are no such intersections, and therefore no Hopf bifurcations, and all of the upper branch of the resonance curve is unstable, if $|\alpha| < \alpha_{1-}$, where α_{1-} is the smaller value of $|\alpha|$ for which (5.13a) has a double root and is approximated by

$$\alpha_{1-} = 1.517[1-0.698\delta^2+O(\delta^4)]. \tag{5.16}$$

A pair of Hopf bifurcations appears to the left of the peak on the upper branch of the resonance curve for $|\alpha| > \alpha_{1-}$, and that segment of this branch between these two bifurcations is stable for $\alpha_{1-} < |\alpha| < \alpha_{3-}$ (see below). A third Hopf bifurcation emerges from the upper turning point to the right of the peak for $|\alpha| = \alpha_{2-}$, where

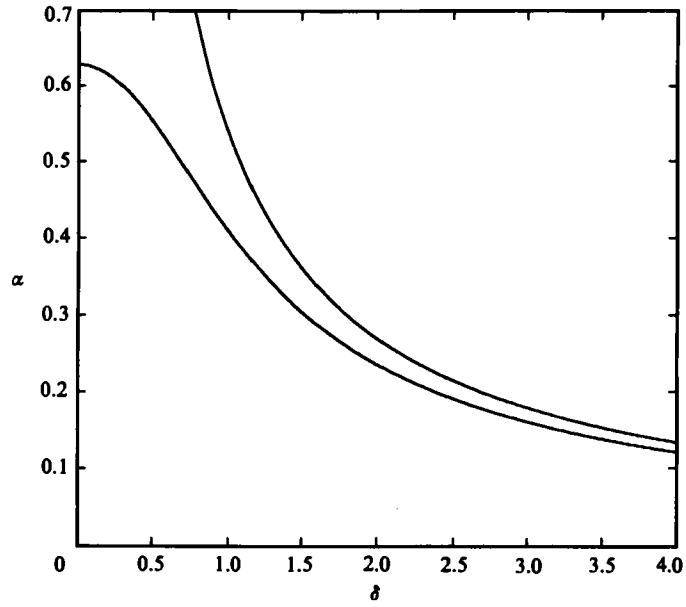

FIGURE 3. The lower curve gives the critical value of $|\alpha|$, α_+, as determined by (5.14), at which a Hopf bifurcation first appears for $\gamma = 1$. The upper curve gives the lower bound of $|\alpha|$ for a single-valued resonance curve.

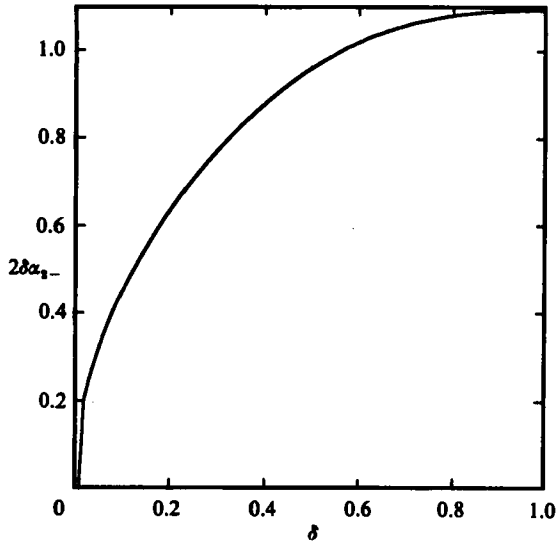

FIGURE 4. The critical value of $|\mu|$, $2\delta\alpha_{2-}$, at which a Hopf bifurcation emerges from the upper turning point for $\gamma = -1$.

α_{2-} is that value of $|\alpha|$ for which the lower branch of the right-hand side of (5.13a) intersects the left-hand side at $R_{\mathrm{H}}^2 = |\alpha|(\alpha^2+\delta^2)^{\frac{1}{2}}$ and is given by (see figure 4)

$$\alpha_{2-} = (2\delta)^{-\frac{1}{2}}\left\{\frac{1+[1+(\delta/\alpha)^2]^{\frac{1}{2}}}{2[1+(\delta/\alpha)^2]}\right\}^{\frac{1}{4}} \tag{5.17a}$$

$$= (2\delta)^{-\frac{1}{2}}[1-\tfrac{3}{8}\delta^3+O(\delta^6)]. \tag{5.17b}$$

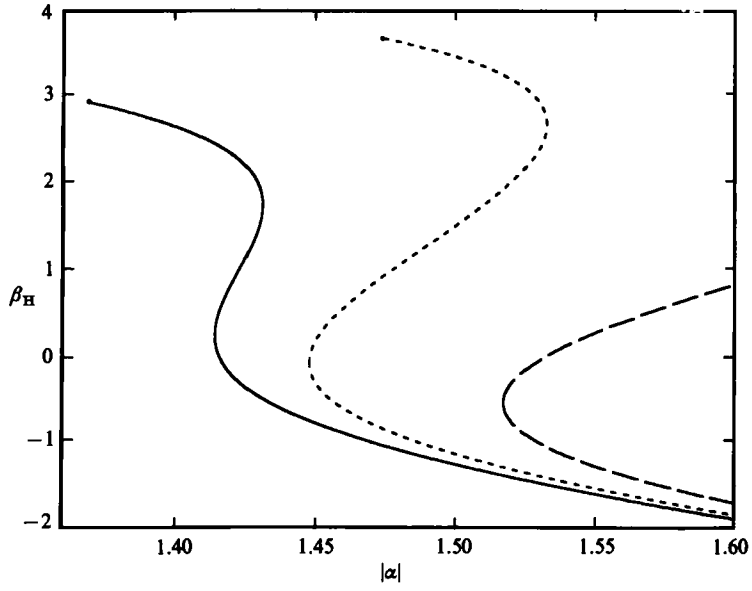

FIGURE 5. The Hopf bifurcations for $\gamma = -1$, $\delta = 0$ (——), 0.25 (– – –) and 0.30 (——). The curves for $\delta = 0.25$ and 0.30 terminate at $|\alpha| = \alpha_{2-}$ (see text and figure 4).

[It follows from (5.17a) that $2\delta\alpha_{2-} \leqslant \mu_c$ ($2\delta\alpha_{2-} = \mu_c$ at $\delta = 3^{\frac{1}{2}}/2^{\frac{5}{6}} = 0.972$), as is necessary for the existence of the turning point.] As $|\alpha|$ increases from α_{2-}, this third bifurcation moves above the turning point to the peak and then down the resonance curve to the left of the peak, where it merges with the higher of the first two bifurcations for $|\alpha| = \alpha_{3-}$, the larger value of $|\alpha|$ for which (5.13a) has a double root, which is approximated by

$$\alpha_{3-} = (2\delta)^{-\frac{1}{2}}[1 + 0.236\delta + O(\delta^2)]. \tag{5.18}$$

That segment of the resonance curve between the turning point and the third bifurcation (as well as that segment between the first two bifurcations) is stable for $\alpha_{2-} < |\alpha| < \alpha_{3-}$, and all of that segment of the resonance curve between the turning point and the remaining bifurcation is stable for $|\alpha| > \alpha_{3-}$.

Numerical calculations (see figure 5) reveal that $\alpha_{1-} < \alpha_{2-} < \alpha_{3-}$ for $0 < \delta < 0.27$, $\alpha_{2-} < \alpha_{1-} < \alpha_{3-}$ for $0.27 < \delta < 0.33$, and α_{1-} and α_{3-} disappear for $\delta > 0.33$. It follows that: the evolution described in the preceding paragraph is valid for $0 < \delta < 0.27$; the first Hopf bifurcation appears at the turning point and there are 0/1/3/1 Hopf bifurcations for $\alpha < \alpha_{2-}/\alpha_{2-} < \alpha < \alpha_{1-}/\alpha_{1-} < \alpha < \alpha_{3-}/\alpha > \alpha_{3-}$ if $0.27 < \delta < 0.33$; there is a single Hopf bifurcation for $\alpha > \alpha_{2-}$ if $\delta > 0.33$.

The Hopf-bifurcation points for $\delta = 0$ (of which there are 0/1 for $|\alpha| \lesssim 0.630$ if $\gamma = 1$ and 0/2 for $|\alpha| \lesssim 1.517$ if $\gamma = -1$) are plotted in figure 6. The lower branch of β_H for $\gamma = -1$ approximates β_H for $\gamma = 1$ for $\alpha \gtrsim 2$, and this remains true for moderate values of δ, for which (5.13) yields

$$\beta_H \sim -\alpha^2 - 4\gamma\alpha^{-4} + O(\alpha^{-10}, \alpha^{-6}\delta^2) \quad (\alpha^2 \uparrow \infty). \tag{5.19}$$

It follows from this and the arguments in the preceding two paragraphs that all of the upper branch of the resonance curve becomes stable for $\alpha^2 \uparrow \infty$ independently of γ and δ.

The solution of (5.13) for $\delta \leqslant \frac{1}{4}$ is indistinguishable (on the scale of the plot) from

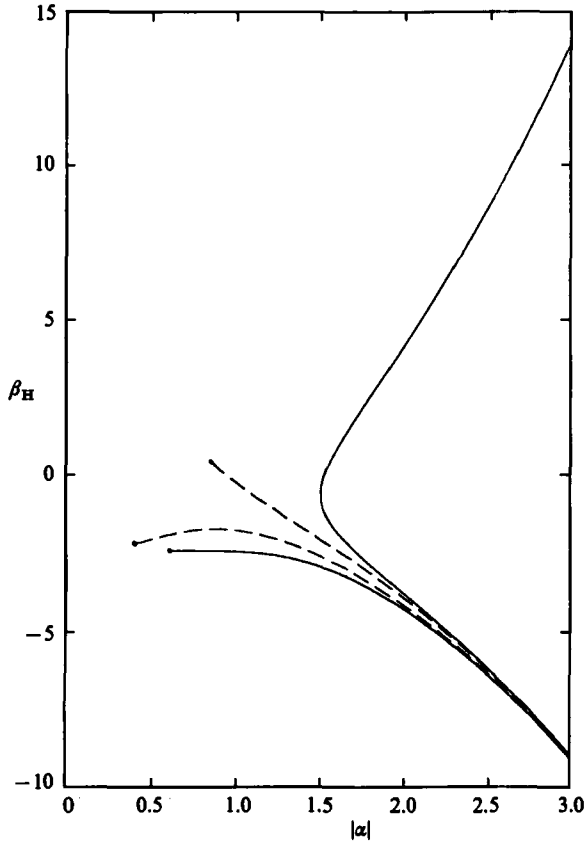

FIGURE 6. The Hopf bifurcations determined by (5.13) for $\delta = 0$ (——) and 1 (– – –) and $\gamma = \pm 1$ (lower/upper curves). The curves for $\gamma = 1$ terminate at $|\alpha| = \alpha_+$ (see text and figure 3). The curve for $\gamma = -1$ and $\delta = 0$ has a branch point at $|\alpha| = \alpha_{1-} = 1.517$). The curve for $\gamma = -1$ and $\delta = 1$ terminates at $|\alpha| = \alpha_{2-}$ (see text and figure 4).

that for $\delta = 0$ for $\gamma = 1$ or along the lower branch for $\gamma = -1$, and this remains true for $\delta \leqslant 1$ except in relatively small neighbourhoods at the end points, but the upper branch for $\gamma = -1$ is a much more sensitive function of δ (it disappears for $\delta > 0.33$), as is evident from the discussion in the penultimate paragraph and from figure 5.

6. Numerical integrations

Numerical integrations of (5.8) and (5.8)* were carried out for some eighty combinations of α, β, γ and δ with various initial conditions. The asymptotic ($\tau \gg 1$) solutions appeared to be relatively insensitive to α and δ insofar as both δ and $|\alpha|\delta$ were small, and the principal variation was in β with $\gamma = 1$ or -1. In that parametric range where stable fixed points exist for $\gamma = 1$, the solutions terminated either on a fixed point or in a simple limit cycle, depending upon the initial conditions. Limit cycles also were obtained on the unstable sides of the Hopf bifurcation; some of these underwent period doubling and period quadrupling, but neither accumulation points nor chaotic motions were found. For $\gamma = -1$, simple limit cycles were obtained in a narrow parametric window on the unstable side of the Hopf bifurcation; all other solutions diverged in the absence of stable fixed points.

I am indebted to Ms Janet Becker and Mr Mark Swenson for aid in the numerical computations. This work was supported in part by the Physical Oceanography Division, National Science Foundation, NSF Grant OCE81-17539, and by the Office of Naval Research under Contract N00014-84-K-0137, NR 062-318 (430).

Appendix A. Surface tension

The potential energy per unit area (in the $\boldsymbol{x}$-plane) due to a uniform surface tension σ is

$$V = \sigma\{[1+(\nabla\eta)^2]^{\frac{1}{2}}-1\} = \sigma[\tfrac{1}{2}(\nabla\eta)^2-\tfrac{1}{8}(\nabla\eta)^4+\ldots]. \tag{A 1}$$

Combining (2.2) and (3.1) in (A 1), averaging over $\boldsymbol{x}$, and subtracting the result from (3.2), we obtain

$$\mathscr{L} = \mathscr{L}(3.2)-\sigma(A_1^2+4A_2^2-\tfrac{3}{4}A_1^4). \tag{A 2}$$

This implies the substitution of

$$B = \frac{1}{2}\left[\frac{\rho_-(3T_-^{-2}-1)(U_--c)^2-\rho_+(3T_+^{-2}-1)(U_+-c)^2}{\rho_\pm(T_\pm+T_\pm^{-1})(U_\pm-c)^2-(\rho_--\rho_+)gk^{-1}-4\sigma k}\right], \tag{A 3}$$

$$c_1^2 = \frac{(\rho_--\rho_+)(g/k)+\sigma k}{\rho_+T_+^{-1}+\rho_-T_-^{-1}}, \tag{A 4}$$

$$C = \frac{\rho_\pm(2T_\pm^{-1}-T_\pm^{-3})(U_\pm-c)^2-\frac{3}{4}\sigma k+B^2[\rho_\pm T_\pm(U_\pm-c)^2-3\sigma k]}{\rho_\pm T_\pm^{-1}(U_\pm-c)^2} \tag{A 5}$$

in place of (3.4), (3.6a) and (3.7); summation over the vertically ordered, alternative signs is implicit in (A 3) and (A 5).

The denominator of B is no longer positive-definite and vanishes for that value of k at which the second harmonic of an interfacial gravity-capillary wave of infinitesimal amplitude resonates with the corresponding fundamental (cf. Nayfeh & Saric 1972; Weissman 1979). The scaling adopted in (4.1) is inappropriate, and the stability problem must be reformulated, in some neighbourhood of this resonance. Moreover, the parameter C may be negative over a wider parametric range, including $kh_\pm = \infty$, than for $\sigma = 0$. It should be observed, however, that the resonance is rather weak if $\rho_--\rho_+ \ll \rho_-+\rho_+$.

Appendix B. Hamiltonian formulation

The usual formalism for the transformation from a Lagrangian to a Hamiltonian formulation (Goldstein 1980, §8.1) for a dynamical system may be placed in the complex form

$$P_n = \frac{\partial L}{\partial \dot{Q}_n^*}, \quad H = P_n\dot{Q}_n^*+P_n^*\dot{Q}_n-L, \tag{B 1a, b}$$

where P_n and Q_n are complex, canonically conjugate coordinates.

Recasting (5.5) in the form

$$\mathscr{L} = \epsilon^4|C_0|(\rho_--\rho_+)gk^{-2}L, \quad A_1 = Q, \tag{B 2a, b}$$

we obtain

$$L = (\dot{Q}+\mathrm{i}\alpha Q)(\dot{Q}^*-\mathrm{i}\alpha Q^*)-(\alpha^2+\beta)QQ^*-\gamma Q^2Q_*^2-(Q+Q^*), \tag{B 3}$$

$$P = \frac{\partial L}{\partial \dot{Q}^*} = \dot{Q}+\mathrm{i}\alpha Q, \tag{B 4}$$

$$H = PP^*+\mathrm{i}\alpha(PQ^*-P^*Q)+(\alpha^2+\beta)QQ^*+\gamma Q^2Q^{*2}+Q+Q^*. \tag{B 5}$$

The counterparts of (5.6) and (5.6)* are

$$\dot{P} = -\frac{\partial H}{\partial Q^*} = -1 - \mathrm{i}\alpha P - (\alpha^2 + \beta) Q - 2\gamma |Q|^2 Q, \tag{B 6a}$$

$$\dot{Q} = \frac{\partial H}{\partial P^*} = P - \mathrm{i}\alpha Q. \tag{B 6b}$$

It follows from (B 6) that $\mathrm{d}H/\mathrm{d}t = 0$ and hence that H is a constant of the motion. Substituting (B 2b) and (B 4) into (B 5), we obtain (5.7).

REFERENCES

ALTMAN, D. B. 1985 Laboratory studies of internal gravity wave critical layers. Ph.D. dissertation, University of California, San Diego.

DRAZIN, P. G. 1970 Kelvin–Helmholtz instability of finite amplitude. *J. Fluid Mech.* **42**, 321–335.

GOLDSTEIN, H. 1980 *Classical Mechanics*. Addison-Wesley.

KEULEGAN, G. H. & CARPENTER, L. H. 1961 An experimental study of internal progressive oscillatory waves. *Natl Bur. Stand. Rep.* 7319.

MASLOWE, S. A. & KELLY, R. E. 1970 Finite amplitude oscillations in a Kelvin–Helmholtz flow. *Intl. J. Non-Linear Mech.* **5**, 427–435.

MILES, J. W. 1986 Weakly nonlinear waves in a stratified fluid: a variational formulation. *J. Fluid Mech.* **172**, 499–512.

NAYFEH, A. H. & SARIC, W. S. 1972 Nonlinear waves in Kelvin–Helmholtz flow. *J. Fluid Mech.* **55**, 311–327.

SAFFMAN, P. G. & YUEN, H. C. 1982 Finite-amplitude interfacial waves in the presence of a current. *J. Fluid Mech.* **123**, 459–476.

STEWARTSON, K. 1981 Marginally stable inviscid flows with critical layers. *IMA J. Appl. Maths* **27**, 133–175.

STOKER, J. J. 1950 *Nonlinear Vibrations*. Interscience.

THORPE, S. A. 1968 A method of producing shear flow in a stratified fluid. *J. Fluid Mech.* **32**, 693–704.

WEISSMAN, M. A. 1979 Nonlinear wave packets in the Kelvin–Helmholtz instability. *Phil. Trans. R. Soc. Lond.* A **290**, 639–685.

YUEN, H. C. 1984 Nonlinear dynamics of interfacial waves. *Physica* **12D**, 71–82.